Cement and Concrete Research 42 (2012) 526–538

Contents lists available at SciVerse ScienceDirect

Cement and Concrete Research

journal homepage: http://ees.elsevier.com/CEMCON/default.asp

Modeling the coupled effects of temperature and fineness of Portland cement on the hydration kinetics in cement paste

Pipat Termkhajornkit *, Rémi Barbarulo

Lafarge Research Centre, 95 Rue de Montmurier 38290 St-Quentin-Fallavier, France

ARTICLE INFO

Article history:
Received 27 July 2010
Accepted 22 November 2011

Keywords:
Hydration (A)
Kinetics (A)
Temperature (A)
Fineness (A)
Cement paste (D)

ABSTRACT

This paper revisits the coupled impacts of fineness and temperature on the kinetics of Portland cement hydration. The approach consists in i) modeling the impact of fineness on cement dissolution through the hypothesis that the surface dissolution rate of cement particles is independent of their size, in order to, in a second step, ii) model the impact of temperature on the kinetics of cement dissolution. The analysis of the experimental results shows that the effect of cement fineness on the hydration kinetics can be captured by a simple hypothesis: for any age, the reacted thickness of cement grains can be considered independent of the initial cement particle size. In addition, the analysis of the results at different temperatures shows that a constant activation energy can account for the effect of temperature on the hydration kinetics, with an Arrhenius equation applied to the kinetics of surface dissolution. The results from the model give a good agreement with the experimental results in a significant number of combinations (different Portland cements, water/cement ratio from 0.5 to 0.6, cement Blaine fineness from 3500 to 6600 cm^2/g, temperature histories between 20 and 60 °C).

1. Introduction

Increasing the rate of hydration of cement is one of the most common ways (with reducing the water/cement ratio) to increase the rate of development of the mechanical properties of concrete. Both temperature and cement fineness change the kinetics of cement hydration. For instance, in the precast concrete industry, thermal treatment is often used to accelerate cement hydration and consequently accelerate compressive strength development — thus increasing the productivity. On the other side, for ready-mix applications, low temperature can lead to low rates of strength development. Another way to increase productivity is to use a more reactive (e.g. finer) cement. Both factors (fineness and temperature) have been studied extensively, but rarely within a same study.

The originality of this work is to propose a simple model that can estimate simultaneously the effects of both temperature and fineness on degree of hydration. The model is based on simple geometrical and physical considerations. It was evaluated on the basis of specific experiments performed on cement pastes, designed to explore the impact of the main parameters considered: cement fineness, temperature history and water/cement ratio.

1.1. Effect of temperature on the kinetics of hydration

The most obvious impact of temperature on concrete properties is the fact that a higher temperature increases early compressive strength and lowers long term compressive strength. This phenomenon was the reason for many studies on the impact of temperature on cement hydration [1–6].

It is largely admitted that at early ages, temperature increases the rate of cement hydration [1,2,4,7–12], justified by the fact that temperature induces faster kinetics of the chemical phenomena (faster dissolution, nucleation or precipitation rates) and faster diffusion through the hydrates assemblage around unreacted cement grains. Many authors have used the Arrhenius equation in order to capture the effect of temperature on the kinetics of hydration; this modeling approach will be detailed further in this paper (Section 2.1).

At later ages, the lower final compressive strength of concretes cured at higher temperature has led some authors to propose that the kinetics of hydration was slowing down after the initial acceleration [1,11,13]. The denser layer of hydration products observed at higher temperature [14,15] or an increased polymerization rate of C–S–H [16] was considered as the reason for a slow down of the diffusion process. However, it is quite largely admitted today that final degrees of hydration are similar at late ages, regardless of temperature of hydration [4,10–12], while the observed lower final strength for concretes cured at higher temperature is induced by a coarser microstructure with denser hydrate layers around the anhydrous products [1,4,8,9,17].

* Corresponding author. Tel.: +33 4 74 82 83 87; fax: +33 4 74 82 80 11.
E-mail address: pipat.termkhajornkit@lafarge.com (P. Termkhajornkit).

0008-8846/$ – see front matter © 2011 Elsevier Ltd. All rights reserved.
doi:10.1016/j.cemconres.2011.11.016

1.2. Effect of cement fineness on the kinetics of hydration

The impact of fineness on cement hydration is more straightforward. Fineness of cement is known to increase significantly the compressive strength, particularly at early ages, and to a lesser extent at later ages [18,19]. This acceleration of strength development is considered to be the result of a faster hydration of cement [20] due to a higher specific surface. The impact of fineness on Portland cement hydration has been studied intensively (e.g. [19–24]) and modeled in many ways [20,25–35].

However, not many experimental and modeling studies focusing on the coupled effects of cement fineness and temperature on cement hydration can be found. The present study was designed to evaluate and model the simultaneous effects of fineness and temperature.

2. Theoretical considerations

2.1. Modeling impact of temperature on hydration kinetics

The impact of temperature on the kinetics of cement hydration is often modeled by an Arrhenius equation, which can be written in a simplified form as:

$$\left(\frac{d\alpha}{dt}\right)_{\alpha=\alpha_0}^{T=T_2} = \left(\frac{d\alpha}{dt}\right)_{\alpha=\alpha_0}^{T=T_1} \times \exp\left\{-\frac{E_a}{R}\times\left(\frac{1}{T_2}-\frac{1}{T_1}\right)\right\} \quad (1)$$

where α is the degree of hydration, E_a is the apparent activation energy (J/mol), R is the gas constant (8.31243 J.mol^{-1}.K^{-1}) and T is the absolute temperature (Kelvin). It should be noted that here the degree of hydration and the apparent activation energy E_a integrate all effects of temperature on the processes of cement hydration, including chemical reactions, diffusion of ions and water, plus restrictions such as space limitation, lack of water, etc.

Eq. (1) implies that knowing the hydration kinetics $\left(\frac{d\alpha}{dt}\right)_{\alpha=\alpha_0}^{T=T_1}$ at degree of hydration α_0 and temperature $T=T_1$, one can compute the hydration kinetics $\left(\frac{d\alpha}{dt}\right)_{\alpha=\alpha_0}^{T=T_2}$ at temperature $T=T_2$, for degree of hydration α_0. The apparent activation energy E_a should be independent of temperature, but is often considered to be dependant on the degree of hydration α in order to fit the experimental data (e.g. [11,36,37]). Some authors report that E_a as defined by Eq. (1) also depends on cement mineralogy and fineness (e.g. [38,39]).

It is worth noting that the Arrhenius equation can be used to estimate the impact of temperature on the rate of a given chemical reaction [40]. Cement hydration involves many different mechanisms (dissolution of cement phases, precipitation of hydrates, diffusion of ions and water) and by such the impact of temperature on the kinetics should not be modeled by a simple Arrhenius equation. But it is rarely mentioned that one of the major reasons why this should not be done is because cement is a powder with a broad particle size distribution [26]. Indeed, as will be demonstrated in Section 2.4, if the surface dissolution rate follows an Arrhenius law, the overall dissolution rate (as measured through degree of hydration) may not follow an Arrhenius law.

2.2. Introduction of the 'uniform reacted thickness' concept

Blaine surface area is probably the simplest and the most classical way to characterize cement fineness. However, such a simple parameter is inadequate for a precise evaluation of the influence of fineness on the degree of hydration. Indeed, a parameter representative only of the initial surface area (such as Blaine or BET) can account only for the very first moments of hydration; the impact of the initial surface area on the kinetics of cement is not relevant anymore once the reactive surface has started decreasing. Similarly, mean diameter such as D50 cannot capture how dissolution affects the reactive surface area. More sophisticated models have also been proposed, that take into account the particle size distribution of cement and in some cases the mineralogy of cement grains [31–34].

In the present work we consider an intermediate approach that takes into account the whole particle size distribution of cement, but with simple hypotheses for what concerns the mechanisms of cement dissolution. Let us consider a mineral which dissolves, at instant t, with a rate $k(t)$ expressed in quantity of matter per unit of surface area and unit of time, so that the quantity of matter dissolved during a small time increment dt is:

$$dn = k(t).S(t).dt \quad (2)$$

where $S(t)$ is the surface area of the mineral at time t. Note that no hypothesis is made concerning the mechanisms that determine the dissolution rate $k(t)$. The variation of volume of the dissolving mineral during time dt is:

$$dV = -V^m.dn = -V^m.k(t).S(t).dt \quad (3)$$

where V^m is the molar volume of the mineral considered.

Now, let us consider a spherical particle of the said mineral, of initial radius $r(0)$. At time t, the radius of the particle $r(t)$ varies of value dr during time dt, and its surface area is $S(t)$, so that $dV=S(t).dr$. By combining this equality with equation Eq. (3), we get:

$$dr = -V^m.k(t).dt. \quad (4)$$

By integrating the previous equation over time, the radius of the particle at time t is given by:

$$r(t) = r(0) - V^m \int_{\theta=0}^{\theta=t} k(\theta).d\theta. \quad (5)$$

We now introduce the notion of 'dissolved depth' or 'reacted thickness' $h(t)=r(0)-r(t)$, i.e. the distance of the dissolving surface from the original surface of the particle, that can be expressed as:

$$h(t) = r(0) - r(t) = V^m \int_{\theta=0}^{\theta=t} k(\theta).d\theta. \quad (6)$$

One can see that, if the dissolution rate $k(t)$ does not depend on the radius of the particle, the right-hand side of equation Eq. (6) is not a function of the initial particle size. Consequently, the reacted thickness at time t should be identical whatever the initial particle size. This hypothesis, referred to as 'uniform reacted thickness' concept in this study, and illustrated in Fig. 1, will be discussed later on in this paper. Note that we also assume that the cement particles are spherical and monophasic, which are clear oversimplifications of the complexity of cement nature.

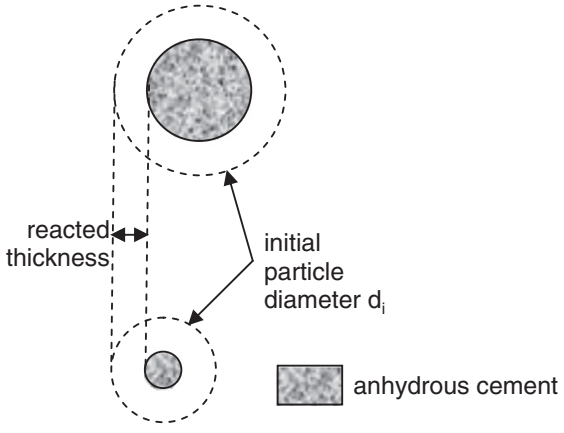

Fig. 1. Schematic representation of the 'uniform reacted thickness' concept.

It is interesting to note that the 'uniform reacted thickness' concept was proposed and applied (although not justified) by Osbaeck and Johansen [20]. This approach is probably the simplest version of the so-called 'shrinking unreacted core model' (e.g. [26,28–30,33,35,41]).

With these assumptions, by integrating over all the classes of the particle size distribution of cement, the degree of hydration $\alpha(t)$ can be expressed as:

$$\alpha(t) = \sum_{i,\ d_i>2h(t)} \left\{ x_i \times \left(1 - \left[1 - \frac{2h(t)}{d_i} \right]^3 \right) \right\} \tag{7}$$

where d_i is the initial diameter and x_i is the volume fraction of particles in particle size distribution class i, $h(t)$ is the reacted thickness at time t and the term in square brackets cannot be less than zero. The numerical applications will be performed later in this paper by integrating the right-hand side of Eq. (7) over all the classes of the particle size distribution of cement.

Thus,

$$\frac{d\alpha}{dt}(t) = \frac{dh}{dt}(t) \times \left\{ \sum_{i,\ d_i>2h(t)} \left[x_i \times \frac{6}{d_i} \left(1 - \frac{2h(t)}{d_i} \right)^2 \right] \right\}. \tag{8}$$

As shown above, $\frac{dh}{dt} = V^m.k(t)$ is related to the kinetics of dissolution of the cement surface, and can be considered as an intrinsic parameter representing the 'reactivity' of cement, independently of its particle size distribution.

2.3. Calculation of the reacted thickness

Direct measurement of reacted thickness of cement particles is not easily achievable, in particular since the initial size of a given hydrated particle is hardly known. It was chosen instead to measure the degree of hydration of cement. Then, the value of the reacted thickness $h(t)$ was computed using a least-square regression between measured and calculated hydration degree (Eq. (8)). In order to evaluate the 'uniform reacted thickness' concept, each cement used in this study was tested at different levels of fineness, up to finenesses rarely encountered in actual industrial cements.

2.4. Combining an Arrhenius equation and 'uniform reacted thickness' concept

Since $\frac{dh}{dt}$ can be assimilated to a rate of surface dissolution, and by making the simplifying hypothesis that cement dissolution is a one-step process, one can apply an Arrhenius equation to this variable [40], so that:

$$\left(\frac{dh}{dt} \right)_{h=h_0}^{T=T_2} = \left(\frac{dh}{dt} \right)_{h=h_0}^{T=T_1} \times \exp\left\{ -\frac{E_a(h_0)}{R} \times \left(\frac{1}{T_2} - \frac{1}{T_1} \right) \right\}. \tag{9}$$

It is worth noting that Eq. (1) (Arrhenius law applied to the overall degree of hydration) may not be directly derived by combining Eq. (9) (Arrhenius applied to dissolution rate) and Eq. (8) (integration of dissolution rate over particle size distribution) in case the reacted thickness is not constant. This implies that Eq. (1) may not be adequate to assess the effect of temperature on the global degree of hydration for a polydisperse powder.

2.5. Computing apparent activation energy

Knowing the function $\frac{dh}{dt}$ at two different temperatures, one can compute the apparent activation energy as:

$$E_a(h_0) = R \frac{T_1 \times T_2}{T_2 - T_1} \mathrm{Ln}\left(\frac{\left(\frac{dh}{dt}\right)_{h=h_0}^{T=T_2}}{\left(\frac{dh}{dt}\right)_{h=h_0}^{T=T_2}} \right) \tag{10}$$

where $\left(\frac{dh}{dt}\right)_{h=h_0}^{T=T_1}$ and $\left(\frac{dh}{dt}\right)_{h=h_0}^{T=T_2}$ are the rates of dissolution at temperature T_1 and T_2, respectively, both measured at reacted thickness h_0.

The experimental approach proposed below was designed to evaluate the relevance of the 'uniform reacted thickness' concept and its capacity to capture the effects of fineness and temperature on cement hydration.

3. Experimental protocols

3.1. Materials

In order to have cements with different levels of fineness, three industrial Portland cements (hereafter designated A, B and C) were chosen for their differences in mineralogy, and either air-classified (designated 'c') or jet-air ground (designated 'g') to reach high levels of fineness. The level of fineness will be designated arbitrarily by '90 μm' (industrial cement), '30 μm' and '20 μm' (finer cements). Particle size distributions (64 classes in this work), measured by laser granulometry in ethanol, are given in Fig. 2.

The physical and chemical properties of cements are given in Table 1. Phase compositions of cements in Table 1 are obtained by X-ray diffraction and Rietveld analysis. As can be seen, the process of classification slightly changes the composition of cement. Note that cements A-g-90 μm and A-c-90 μm are two different samples from a same cement plant. The results will show that these differences can be neglected at first order.

3.2. Preparation of cement paste samples and designation of specimens

The degree of hydration of cement was measured by two different methods. For early ages (up to 1–2 days), isothermal calorimetry (TAM Air calorimeter) was used. For later ages (1 h–28 days), the degree of hydration was measured by coupling X-ray diffraction and Rietveld analysis associated to bound-water measurements. Details of methods and calculations are given below (§ 3.3 and 3.4).

Three temperatures were considered in this study: 20, 40 and 60 °C, in order to remain below ~70 °C, temperature for which equilibrium of calcium sulfoaluminate phases is systematically modified [42]. The experimental conditions are summarized in Table 2. Additionally, three different heat-curing cycles between 20 and 60 °C were applied, as illustrated in Fig. 3.

All materials and apparatuses were pre-conditioned at the required temperature. Water and cement were mixed for 60 s at 3000 rpm. Paste spread on the mixer bowl was put back in the mix. Then cement paste was further mixed for 60 s at 3000 rpm. The fresh cement paste was poured into 7.4 mm diameter and 22.7 mm height waterproof molds. To prevent segregation, the molds were continuously rotated for one night in a water bath at desired temperature. After that, the samples were demolded and kept in lime saturated water at the desired temperature until testing. The properties of samples, namely degree of hydration, porosity and compressive strength were measured at ages up to 28 days. This paper deals with degree of hydration only.

The names of specimens were given according to the designation of cements (A, B and C) – classified or ground indication (c and g,

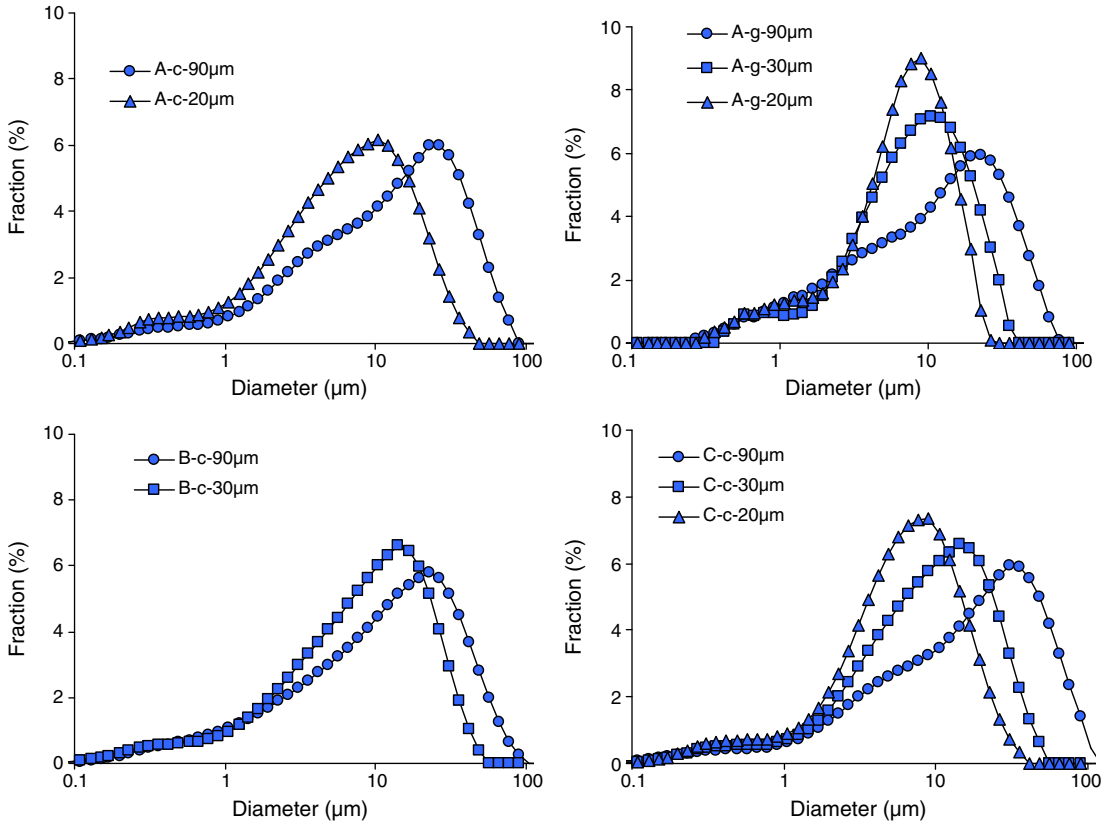

Fig. 2. Particle size distributions of cements used in this study (volume fractions).

respectively) – fineness (90 μm, 30 μm and 20 μm are initial (industrial), smaller than 30 μm and smaller than 20 μm, respectively) – curing temperature (20 °C, 40 °C and 60 °C). For example, A-c-30 μm-40 °C means cement A – classified below 30 μm – paste cured at 40 °C, respectively.

3.3. Determination of hydration degree by isothermal calorimetry

Cement pastes made with classified cements were tested at 20 °C and 40 °C and cement pastes made with ground cement were measured at 20 °C. The water/cement ratio was 0.5 by weight. The specimens were mixed inside the calorimeter, at two temperatures, 20 and 40 °C. Hydration was followed continuously for at least 24 h. The heat flux was normalized by the weight of cement and the cumulative heat was calculated by integrating the heat flux. The starting point of integration was fixed at the lowest heat flux value between the first peak and the second peak.

The degree of hydration can be calculated with the following equation:

$$\alpha(t) = \frac{H(t)}{H_{final}} \tag{11}$$

where $\alpha(t)$ is the degree of hydration of cement at time t, $H(t)$ (J/g of cement) is the cumulative heat flow at time t and H_{final} (J/g of

Table 1
Physical properties and mineralogical composition of cements used.

Cement	Classified cement A		Classified cement B		Classified cement C			Ground cement A		
	A-c-90 μm	A-c-20 μm	B-c-90 μm	B-c-30 μm	C-c-90 μm	C-c-30 μm	C-c-20 μm	A-g-90 μm	A-g-30 μm	A-g-20 μm
Blaine specific surface area (cm2/g)	3950	6180	4300	4930	3570	4950	6630	3960	NA	6630
Density (g/cm3)	3.13	3.09	3.15	3.16	3.10	3.09	3.08	3.15	3.17	3.12
Alite (%)	60.3	59.5	67.9	66.2	70.1	70.8	67.9		62.7	
Belite (%)	17.2	13.2	12.3	14.1	10.3	8.2	9.1		16.2	
Ferrite (%)	4.6	4.7	5.6	5.5	2.5	3.3	3.4		5.1	
Aluminate (%)	7.8	9.4	9.0	9.0	10.8	10.1	10.2		7.8	
Lime (%)	0.2	0.1	0.6	0.0	0.3	0.3	0.1		0.2	
Periclase (%)	0.3	0.3	1.0	0.8	0.2	0.3	0.4		0.3	
Anhydrite (%)	1.5	3.4	1.4	1.9	0.7	0.7	1.2		2.1	
Hemihydrate (%)	1.8	1.0	1.3	2.2	1.8	2.3	3.0		1.0	
Gypsum (%)	2.5	2.6	0.0	0.0	2.0	2.8	2.9		1.9	
Calcite (%)	2.3	5.1	0.0	0.0	0.7	0.3	0.9		2.2	
Portlandite (%)	0.0	0.1	0.7	0.2	0.5	0.6	0.6		0.1	
Quartz (%)	0.3	0.7	0.0	0.1	0.2	0.3	0.3		0.1	

Table 2
Experimental conditions.

Cement	Fineness	Temperature	W/C	Measurement of hydration degree
A	Initial	20, 40 °C	0.50	Isothermal calorimetry
	Classified<30 μm	20, 40 °C	0.50	Isothermal calorimetry
	Classified<20 μm	20, 40 °C	0.50	Isothermal calorimetry
B	Initial	20, 40 °C	0.50	Isothermal calorimetry
	Classified<30 μm	20, 40 °C	0.50	Isothermal calorimetry
	Classified<20 μm	20, 40 °C	0.50	Isothermal calorimetry
C	Initial	20, 40 °C	0.50	Isothermal calorimetry
	Classified<30 μm	20 °C	0.50	Isothermal calorimetry
	Classified<20 μm	20 °C	0.50	Isothermal calorimetry
A	Initial	20, 40, 60 °C	0.50	Rietveld
A	Ground<30 μm	20 °C	0.50	Rietveld
A	Ground<20 μm	20 °C	0.50	Rietveld
A	Initial	20 °C	0.33	Rietveld
A	Ground<20 μm	60 °C	0.60	Rietveld
A	Initial	Cycle 1, cycle 2, cycle 3	0.50	Rietveld

cement) is the cumulative heat flow when the reaction is completed, which can be calculated by the following equation:

$$H_{final} = \text{Alite} \times H_{f-\text{Alite}} + \text{Belite} \times H_{f-\text{Belite}} + \text{Aluminate} \times H_{f-\text{Aluminate}} + \text{Ferrite} \times H_{f-\text{Ferrite}} \quad (12)$$

where Alite, Belite, Aluminate and Ferrite are the fractions by weight of the four main phases of anhydrous cement, as determined by Rietveld XRD, and H_f are the respective heat of hydration of Alite, Belite, Aluminate and Ferrite, assumed equal to 517, 262, 1453 and 725 J/g, respectively [43]. It is also worth noting that this calculation is based on the simplified assumption that all clinker phases react with the same kinetics.

3.4. Measurement of degree of hydration on stopped cement paste samples

After measurement of compressive strength, broken specimens were put in acetone for 15 min. Then the specimens were removed from acetone and vacuum-dried for 24 h, then ground below 63 μm and used to measure the hydration degree by coupling XRD/Rietveld and bound water.

XRD scans were collected with CuKα radiation over the range $2\theta = 5°–65°$ ($2\theta = 1°$/min). Panalytical Highscore Plus version 2.2.2 software was used to run Rietveld refinements. The total amorphous content in a sample was quantified indirectly by using an external standard. Bound water was measured by multi-element gas analyzer Pyro-Analyser Fractel MIR 9000.

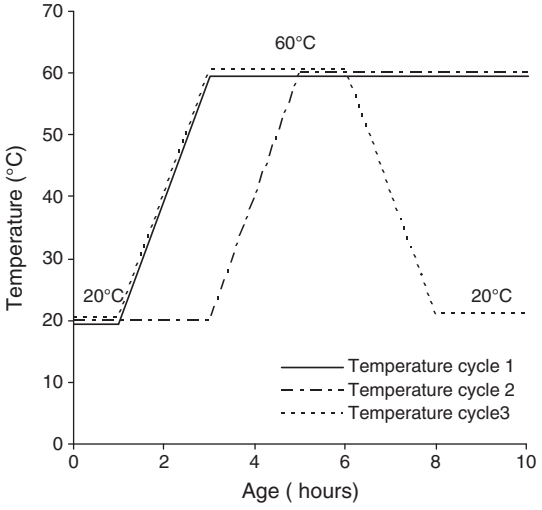

Fig. 3. Temperature cycles 1, 2 and 3.

Hydration degree calculated by XRD/Rietveld analysis and bound water is given by the following equation:

$$\alpha = 1 - \frac{x(t)}{(1-w_n)} \quad (13)$$

where α is hydration degree of cement, w_n is bound water, and $x(t)$ is the residual anhydrous cement in the hydrated sample. It should be noted that Rietveld analysis, in fact, gives the quantity of each phase of the cement paste. However, in this study a global definition of degree of hydration only was used. Note also that bound water in anhydrous cement was neglected.

4. Results

4.1. Impact of fineness and temperature on kinetics of cement hydration

Fig. 4 shows the hydration degree of classified cements measured by isothermal calorimetry. As expected, finer cements hydrate faster and temperature accelerates hydration.

Fig. 5 compares the results from isothermal calorimetry and those from XRD/Rietveld analysis of ground cement A (90 μm, 30 μm and 20 μm). At early age (before 8 h) the degree of hydration from Rietveld analysis is higher than from isothermal calorimetry. This difference could originate from the fact that the ability of XRD/Rietveld to quantify amorphous phases is low when the amount of amorphous phases is low, implying higher errors on hydration degree at early ages. Another hypothesis could be that the method used to stop hydration prior to XRD was not fast enough and hydration continues somehow. Nevertheless, both methods converge after 8 h (or $\alpha > 0.3$). Both methods will be used further, mainly calorimetry before 1–2 days and Rietveld after 8 h. Similar results were obtained at 40 °C, allowing using both methods for degree of hydration above about 0.1.

Fig. 6 shows hydration degree from XRD/Rietveld as a function of time at three different temperatures. Again, temperature accelerates hydration of cement, and until about 28 days, time for which the hydration degrees of samples cured at 20 °C, 40 °C and 60 °C are almost the same, about 0.9. This result is in agreement with data reported by several authors [4–6,12], showing that the dense layer of hydrated products formed at high temperature [4,14] does not limit the final value of hydration degree, as it is sometimes suggested [1,11,13].

4.2. Application of the 'uniform reacted thickness' concept

On the basis of the measured degree of hydration, one can calculate the theoretical reacted thickness as explained in Section 2.3. Fig. 7 shows at 20 and 40 °C: on the left, the reacted thickness of classified cements as calculated from results of isothermal calorimetry; on the right, the degree of hydration, as recalculated from Eq. (7) (reacted thickness is considered identical for each cement fineness). Conclusions are the same for both temperatures. Although the reacted thicknesses calculated individually are not exactly the same for each level of fineness of a given cement, the calculated values of reacted thickness stand within +/− 15% of calculated 'best fit' value (i.e. reacted thickness giving the best fit for all levels of fineness). Moreover, the recalculated degree of hydration is very close to the measured degree of hydration. From these results, it seems that the 'uniform reacted thickness' concept is relevant at early ages (before one day), at 20 and 40 °C, for at least three different cements.

In order to evaluate the model at later ages, the results from XRD/Rietveld were treated in the same way (Fig. 8 (left)). Results show

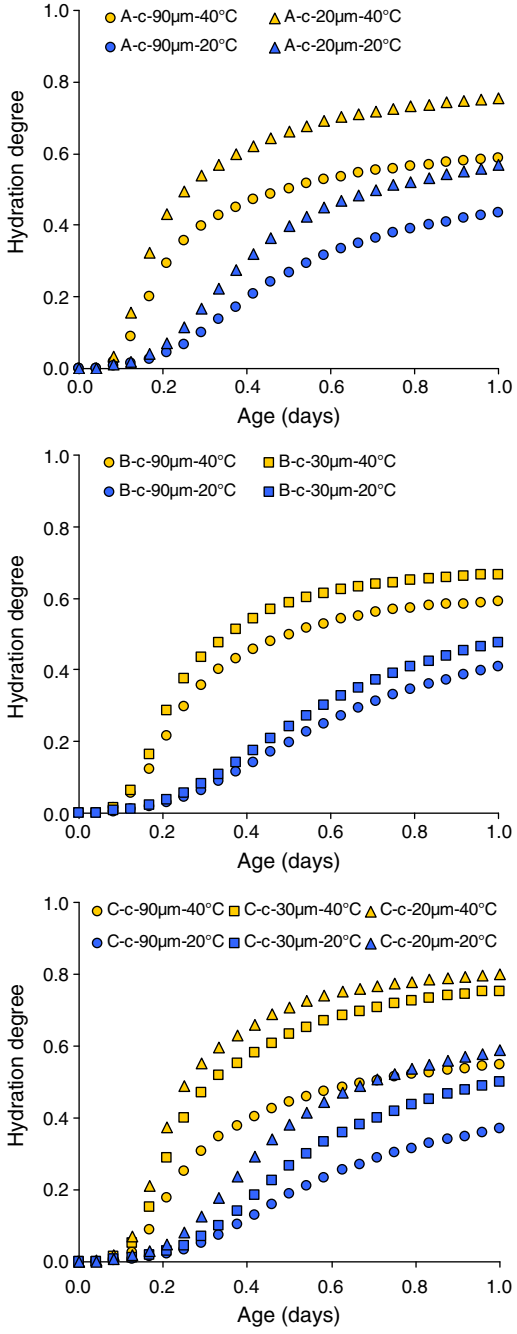

Fig. 4. Hydration degree of classified cement measured by isothermal calorimetry, 20 and 40 °C.

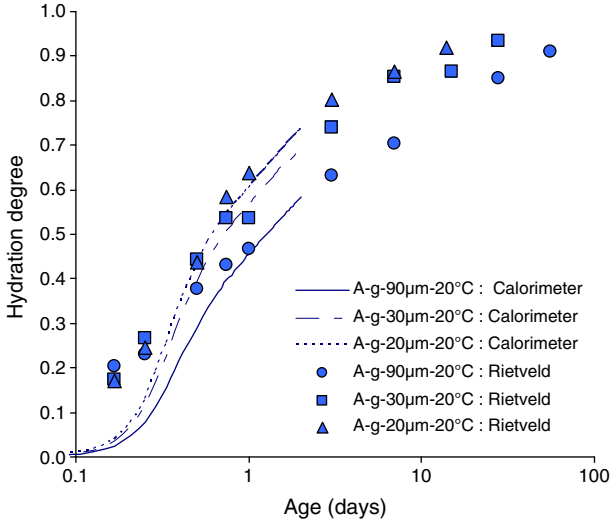

Fig. 5. Hydration degree from XRD/Rietveld and calorimeter; Ground cement A at 20 °C.

that the calculated reacted thickness is independent of cement fineness until about 3–7 days. The values of reacted thickness are of the same order of magnitude of those found by Anderegg and Hubbell (0.4–0.47 μm at 1 day, 1.7–2.6 μm at 7 days and 3.5–5.4 μm at 28 days) [25], although lower than that of Scrivener (3 μm at 40 h) [24], but since these data are already quite scattered it is difficult to conclude. Note that for degrees of hydration close to 1, calculation of reacted thickness becomes less accurate (a variation in reacted thickness has no impact on the degree of hydration when all particles are dissolved; see Appendix, Uncertainty on estimation of reacted thickness). However, Fig. 8 (right) shows that the results from calculations give a reasonable fit with the experimental results when comparing the measured and computed degrees of hydration on the basis of a 'best fit' reacted thickness (i.e. giving best results whatever the fineness). From these results, it seems that the 'uniform reacted thickness' concept is also relevant at later ages (1 h–28 days) at 20 °C.

4.3. Modeling the impact of temperature by combining the 'uniform reacted thickness' concept with an Arrhenius equation

In order to be able to manipulate more easily the data from the previous experiments, the following equation, giving a good fit for reacted thickness as a function of time, is proposed:

$$h(t) = \eta \exp\left(-\left(\frac{t}{\tau}\right)^{-p}\right) \tag{14}$$

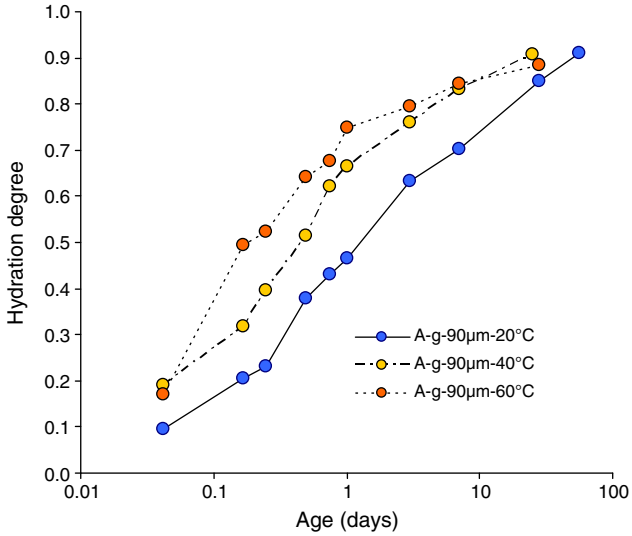

Fig. 6. Hydration degree from XRD/Rietveld coupled with bound water as a function of temperature and age; Ground cement A at 20 °C, 40 °C and 60 °C.

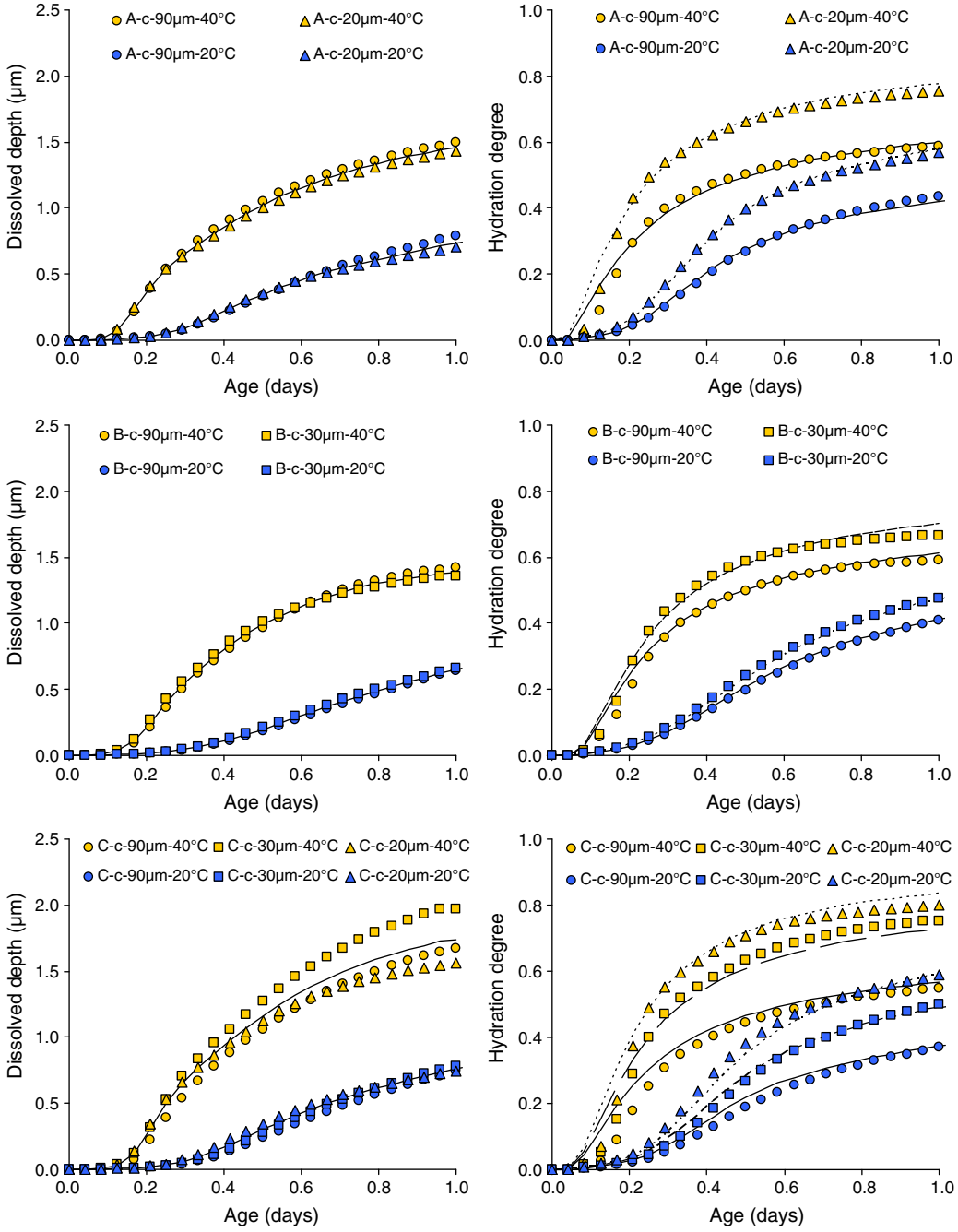

Fig. 7. Reacted thickness calculated from the particle size distribution and hydration degree from isothermal calorimetry; classified cements at 20 and 40 °C. Left: reacted thickness (dots: computed from measured degree of hydration for each cement fineness; lines: value obtained using least-square regression for all 3 cement finenesses simultaneously). Right: hydration degree (dots: measured; lines: computed from reacted thickness).

where h is reacted thickness, t is time and η, τ and p are fitting parameters characteristic of the dissolution kinetics of the cement considered. Note that this equation is used for the sole objective of fitting experimental data and does not intend to model cement hydration.

The derivative of h can be expressed as:

$$\frac{dh}{dt}(t) = \left[\eta \exp\left(-\left(\frac{t}{\tau}\right)^{-p}\right)\right] \times \left[\left(\frac{p}{\tau}\right)\left(\frac{t}{\tau}\right)^{(-p-1)}\right] = h(t) \times \left[\left(\frac{p}{\tau}\right)\left(-Ln\left(\frac{h(t)}{\eta}\right)\right)^{\left(\frac{p+1}{p}\right)}\right]. \quad (15)$$

By combining Eq. (10) and Arrhenius equation (Eq. (15)), one can express the apparent activation energy as:

$$E_a(h = h_0) = R\frac{T_1 \times T_2}{T_2 - T_1} \mathrm{Ln}\left(\frac{\left(\frac{p_2}{\tau_2}\right)\left(-Ln\left(\frac{h_0}{\eta_2}\right)\right)^{\left(\frac{p_2+1}{p_2}\right)}}{\left(\frac{p_1}{\tau_1}\right)\left(-Ln\left(\frac{h_0}{\eta_1}\right)\right)^{\left(\frac{p_1+1}{p_1}\right)}}\right) \quad (16)$$

where η_i, τ_i and p_i are the fitting parameters defined above determined for temperature T_i $(i = 1, 2)$. One can see that, as hydration proceeds, h_0

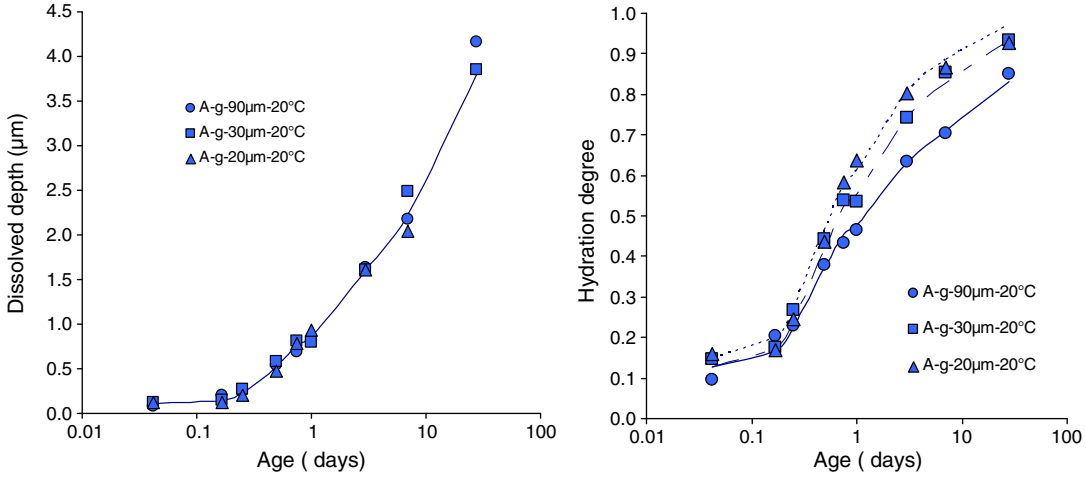

Fig. 8. Reacted thickness and hydration degree for cement A, ground at different finenesses, hydrated at 20 °C. Left: calculated reacted thickness (dots) and 'best fit' value for the 3 finenesses (line); right: degree of hydration measured (dots) and calculated from 'best fit' value (lines).

will increase, implying that E_a will be a function of time (or degree of hydration).

However, as demonstrated in Appendix, Justification of the assumption of equality for the fitting parameters η and p, it is more relevant to consider that the fitting parameters η_i and p_i are independent of temperature ($\eta_1=\eta_2=\eta$ and $p_1=p_2=p$), otherwise the activation energy tends toward $\pm\infty$ when $h(t)\rightarrow\min(\eta_1,\eta_2)$, which has no physical meaning. Consequently, Eq. (16) can be simplified as follows:

$$E_a = R\frac{T_1\times T_2}{T_2-T_1}\times \mathrm{Ln}\left(\frac{\tau_1}{\tau_2}\right) \tag{17}$$

in which case E_a is constant, i.e. independent of time, reacted thickness or degree of hydration.

The following procedure was followed: on the basis of the degree of hydration measured by isothermal calorimetry for each temperature considered, the reacted thickness was calculated using Eq. (7). Then a set of parameters η and p (independent of temperature) and τ (function of temperature of experiment) was adjusted in order to fit experimental data, using a least-square regression method. This finally allows calculation of activation energy according to Eq. (17).

Fig. 9 reports the impact of temperature on the rate of dissolution (measured by isothermal calorimetry) and the calculated activation energy (left), and compares measured and modeled degree of hydration (right). Activation energies ranging from 35 to 45 kJ/mol are found. These values are similar to what is generally reported (30–55 kJ/mol [36,44–47]). There still is a good agreement between measured and calculated degree of hydration for the cements tested, although the induction period is not captured perfectly due to the use of Eq. (14) and the low degree of freedom in fitting parameters since $\eta_1=\eta_2=\eta$ and $p_1=p_2=p$.

A similar approach was used at later ages. Fig. 10 shows that the use of Eq. (14) and the assumption $\eta_1=\eta_2=\eta$ and $p_1=p_2=p$ allow a very good fit of experimental data for reacted thickness at 20, 40 and 60 °C. On this basis, it was possible to calculate the activation energy (about 36 kJ/mol, Fig. 11).

Then integrating over the particle size distribution of the cement (Eq. (7)) allows modeling with a very satisfactory accuracy the impact of temperature on degree of hydration, as illustrated in Fig. 12.

These results show that the concept of apparent activation energy, when applied to the kinetics of dissolution (here expressed by the descriptor 'reacted thickness'), can capture, in addition to the effects of cement fineness, the effects of temperature on cement hydration. The model is also more robust than the traditional application of an Arrhenius equation to the overall rate of hydration since one can use a constant apparent activation energy (i.e. independent of degree of hydration, temperature and cement fineness).

4.4. Evaluation of the model in different conditions

In the previous sections, the model was evaluated and the input parameters (η, τ, p, E_a) were calibrated on the basis of results of experiments varying either fineness or temperature. In this section, both fineness and temperature were modified, and the experimental results obtained on cement A are compared to the model calibrated in the previous sections.

4.4.1. Combining higher water/cement ratio, higher fineness of cement and higher temperature

In order to evaluate the robustness of the model, the following experiment was performed, combining a modification of temperature and fineness: cement A-g-20 µm was hydrated at a curing temperature of 60 °C. Since at this temperature it was very difficult to mix cement with water at w/c = 0.50, a higher water/cement ratio of 0.60 was used. The hydration degree was measured by XRD/Rietveld analysis coupled with bound water until degree of hydration was about 0.90.

The model developed in the previous sections was used to predict the degree of hydration. The kinetics parameters and apparent activation energy determined previously (as for Fig. 12) were used. As shown in Fig. 13, the model gives a very reasonable agreement with the results from the experiment. Once calibrated, the model appears to be able to predict simultaneous modifications of temperature, fineness and water/cement ratio, which allows believing in a certain robustness of the model.

4.4.2. Lower water/cement ratio

It is known that if the w/c ratio is below the stoichiometric value needed for cement hydration, the hydration kinetics will be slowed down [48] and the complete hydration of cement cannot be achieved [49]. Fig. 14 compares the degree of hydration of cement A-g-90 µm cured at 20 °C, w/c = 0.33 or w/c = 0.50. The model gives satisfying results up to about 70% hydration. The slow-down of hydration kinetics at lower w/c, imputable to lack of space for hydration products or to lower availability of water, cannot be captured by the model developed in the previous sections. The limit of validity of the model is not

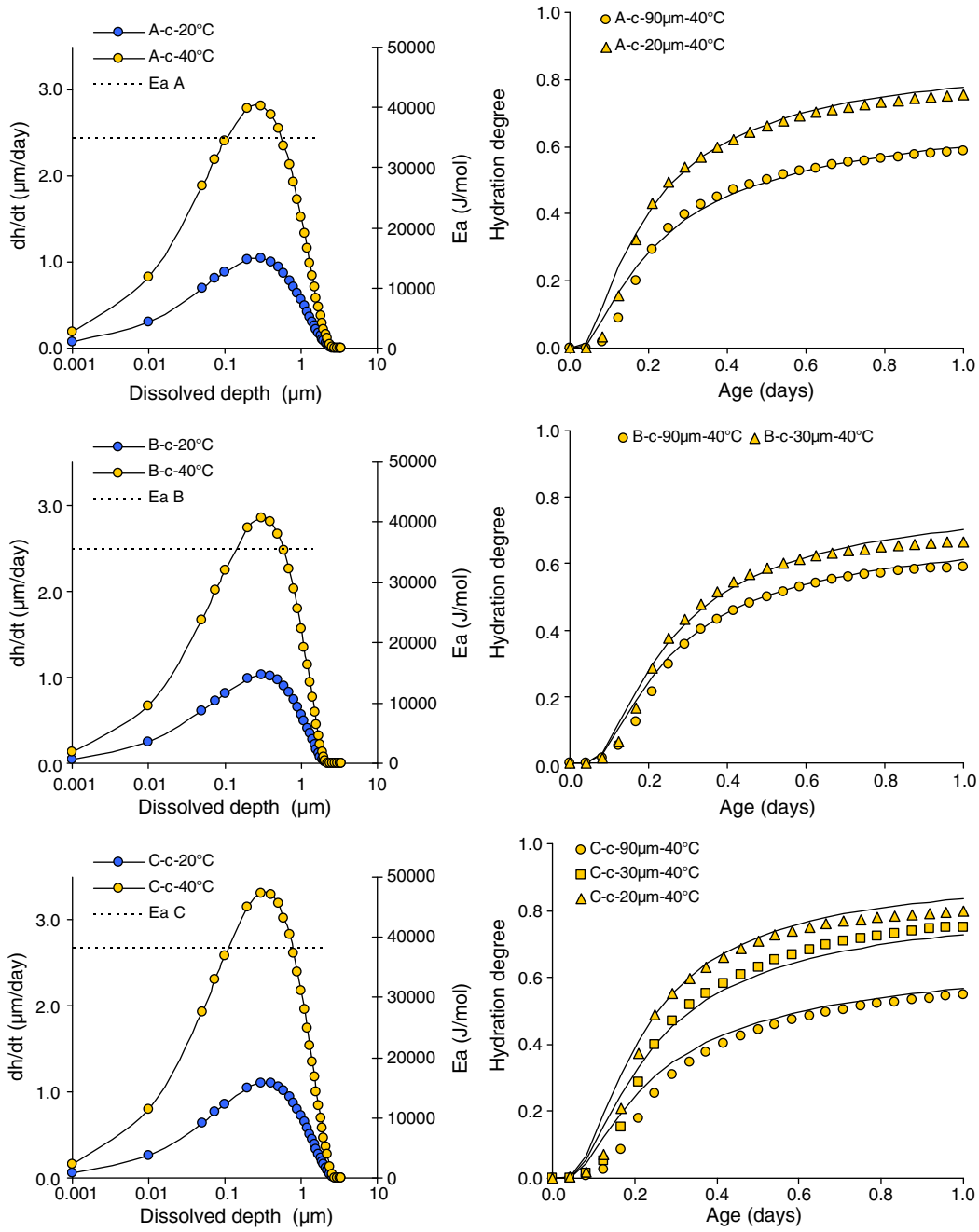

Fig. 9. Rate of surface dissolution $\frac{dh}{dt}$ and degree of hydration for 3 cements; impact of fineness and temperature. Left: rate of dissolution at 20 and 40 °C, and calculated activation energy; right: comparison between degrees of hydration measured (dots) and modeled (lines).

determined, but it seems relevant, in terms of w/c, between 0.50 and 0.60, and loses its accuracy somewhere below 0.50. More sophisticated models should be used for such situations, such as [31–34].

4.4.3. Temperature cycles

The model was used to model the impact of three temperature cycles as described in Fig. 3. For temperature cycle 1, samples were precured at 20 °C for 1 h, then the temperature was increased to 60 °C within 2 h, then kept constant at 60 °C until time of testing. Temperature cycle 2 is similar to temperature cycle 1, except for the fact that the precure period at 20 °C was extended from 1 h to 3 h. Temperature cycle 3 starts like the temperature cycle 1 but after 6 h, the temperature was decreased until 20 °C within 2 h and then kept constant at 20 °C until time of testing. Fig. 15 compares the experimental results (degree of hydration) and the computed results. Again, the results from the model give good agreement with the results from the experiment. As for the tests performed at constant temperature, the model is able to capture very accurately the impact of a non-constant temperature.

5. Discussion on the 'uniform reacted thickness' concept

A strong hypothesis used in the present study is that the reacted thickness of each cement particle is independent of its initial size. As demonstrated in Section 2.2, this hypothesis is equivalent to considering that the surface dissolution rate $k(t)$ does not depend on the radius of the particle. The experimental data generated in this

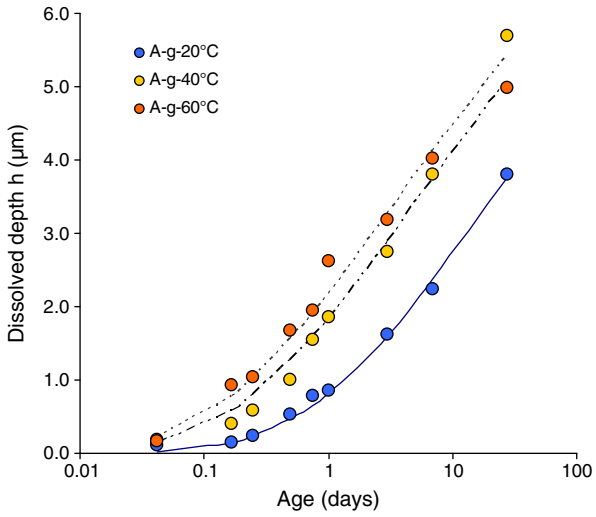

Fig. 10. Comparison of measured (dots) and modeled (lines) values of reacted thickness, on the basis of Eq. (14) and the simplified assumption $\eta_1 = \eta_2 = \eta$ and $p_1 = p_2 = p$.

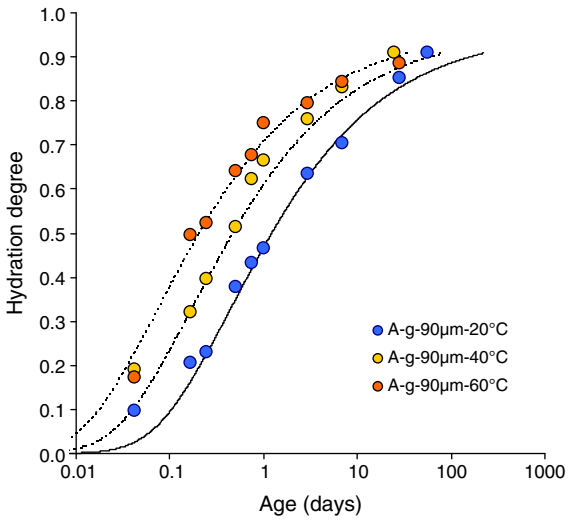

Fig. 12. Comparison of measured (dots) and modeled (lines) values of degree of hydration, using a constant apparent activation energy and combining Eqs. (7), (9) and (14).

study does not disprove this hypothesis, over a significant range of cement compositions, cement finenesses, water/cement ratios and temperature histories.

No hypotheses were made concerning the mechanisms determining the dissolution rate $k(t)$. However, if all particles, whatever their size, exhibit a same surface dissolution rate, this leads to the conclusion that the parameters driving the dissolution rate are 'global' and not 'local' — at least not radius-dependent. Dissolution, driven by the concentrations in the interstitial solution (all particles perceiving the same environment), could be one of these 'global' mechanisms. On the opposite, diffusion through the hydrates assemblage around the unreacted cement grains may depend on the thickness of the hydrated layer, which is function of the initial cement particle size. The authors think that the examples generated in this study do not permit to conclude on these mechanisms; however, it was shown that the 'uniform reacted thickness' concept, equivalent to a dissolution rate $k(t)$ independent on the initial particle size, was sufficient to capture most of the experimental data generated in this study. Only real measurements of reacted thickness could validate this hypothesis.

6. Conclusions

In this study, the effects of cement fineness and temperature on kinetics of cement hydration were investigated, and modeled with simple assumptions. The experimental and modeling results are summarized below.

- For a same age, the hydration reaction was always faster when the curing temperature was higher. This implies that a higher temperature (up to 60 °C) will not limit the final degree of hydration.
- A 'uniform reacted thickness' concept was developed and applied to model the dissolution of cement powder. This very simple assumption states that at a given age, the reacted thickness of cement grains is the same for all grain sizes. The results show

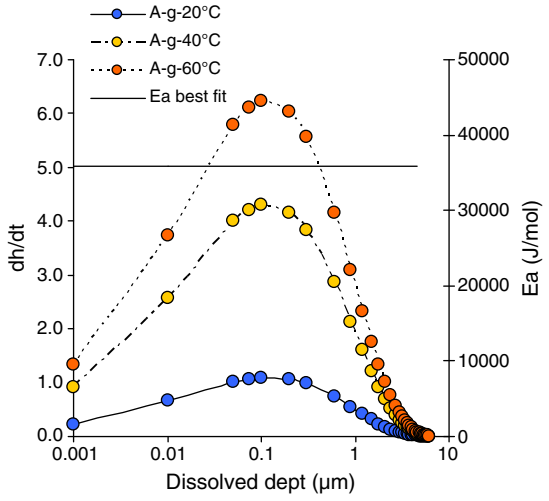

Fig. 11. Calculation of the apparent activation energy, using Eq. (17).

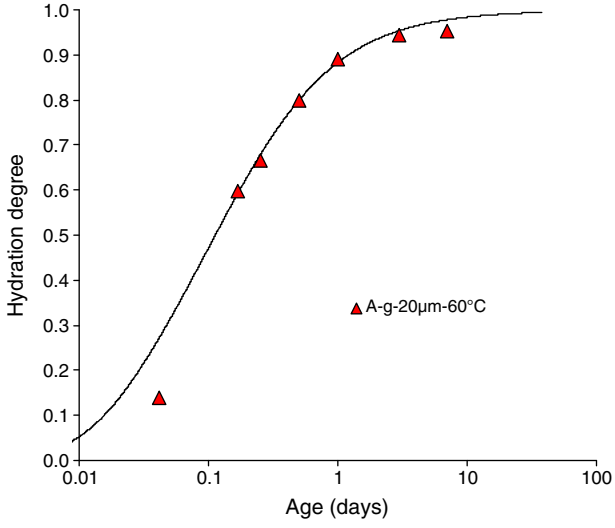

Fig. 13. Comparison between calculated (line) and measured (dots) degree of hydration for cement A-g-20 µm cured at 60 °C, w/c = 0.60.

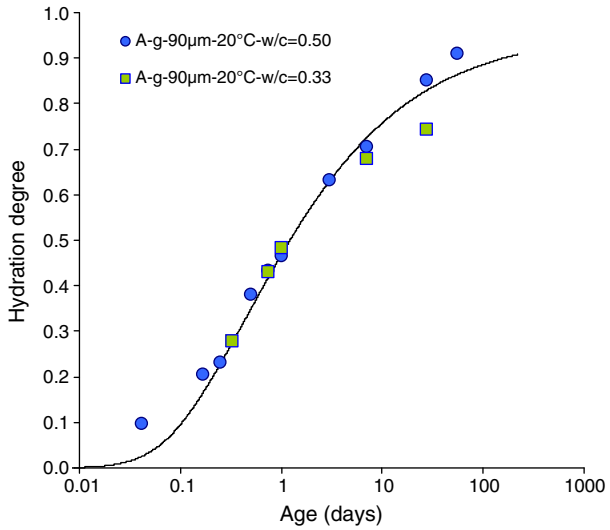

Fig. 14. Comparison of the evolution of the degree of hydration at w/c ratio of 0.50 and 0.33. Solid line = model at 20 °C.

that such a simple hypothesis, integrated over the particle size distribution of cement, can capture adequately the impact of cement fineness on the hydration kinetics.

- It was shown that this concept is equivalent to the hypothesis that the surface dissolution rate is independent on the initial particle size (e.g. all unreacted surfaces of cement grains dissolve at the same rate).
- The effect of temperature on the rate of dissolution of cement can be described very well by applying Arrhenius equation to the kinetics of surface dissolution (expressed here with the 'reacted thickness' variable).
- Moreover, with this formalism, the apparent activation energy can be considered constant (independent of time and temperature, from 20 to 60 °C). The fact that one can consider the apparent activation energy constant over time makes the model easier to use for practical industrial implications.
- The model was evaluated in various conditions, and seems to apply for a temperature range from 20 to 60 °C (constant temperature or temperature cycle), for a cement fineness from d97 = 20 to 90 μm, and w/c from 0.50 to 0.60. For lower w/c (e.g. 0.33), it was shown that such a simplistic model is not able to capture the changes in hydration kinetics due to lack of space or water.

The model appears promising and once calibrated for a given cement, can be used to assess the effects of cement fineness and temperature on the rate of hydration. However, further work should be done, based on this simple hydration kinetics model, in order to better understand and model the impact of fineness and temperature on the rate of strength development.

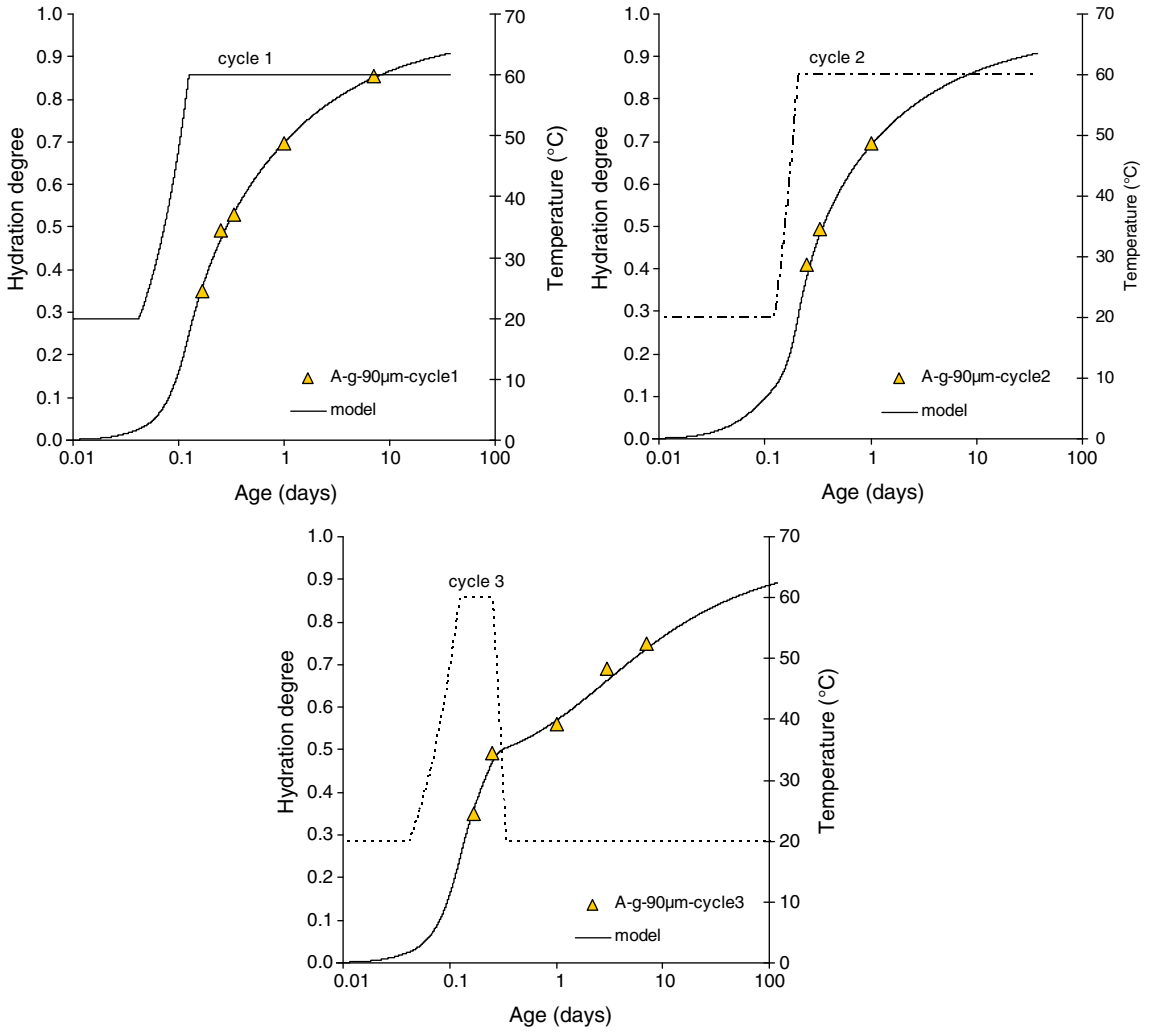

Fig. 15. Comparison of the evolution of the degree of hydration during three different temperature cycles. Dots = experimental results; solid line = model.

Appendices

Uncertainty on estimation of reacted thickness

In this section we estimate the uncertainty induced when computing the reacted thickness as a function of the experimental error on degree of hydration α. Eq. (8) gives:

$$dh = \frac{d\alpha}{\sqrt{n}} \left\{ \sum_{i,\ d_i > 2h(t)} \left[x_i \times \frac{6}{d_i} \left(1 - \frac{2h(t)}{d_i} \right)^2 \right] \right\}^{-1} \tag{18}$$

where n stands for the number of measurements used to determine dh (typically: $n=3$ for 3 different cement finenesses). From which, knowing the uncertainty on the degree of hydration $d\alpha=0.05$ (at 28 days, estimated on the basis of repeatability experiments), one can compute dh. Finally, Table 3 gives some examples showing how dh depends on h.

Justification of the assumption of equality for the fitting parameters η and p

Eq. (16) can be developed as:

$$E_a(h=h_0) = R\frac{T_1 \times T_2}{T_2 - T_1} \left[\mathrm{Ln}\left(\frac{\left(\frac{p_2}{\tau_2}\right)}{\left(\frac{p_1}{\tau_1}\right)} \right) + \left(\frac{p_2+1}{p_2} \right) \times \mathrm{Ln}\left(-\mathrm{Ln}\left(\frac{h_0}{\eta_2} \right) \right) - \left(\frac{p_1+1}{p_1} \right) \times \mathrm{Ln}\left(-\mathrm{Ln}\left(\frac{h_0}{\eta_1} \right) \right) \right].$$

In the following we consider $T_2 > T_1$ (the opposite hypothesis would lead to symmetrical conclusions). We show below that if $\eta_1 \neq \eta_2$ or $p_1 \neq p_2$, then when the reacted thickness tends to its maximum value η_1 or η_2, the activation energy E_a tends to $\pm\infty$, which is not relevant.

In case $\eta_1 > \eta_2$, as h_0 tends to η_2, we write $h_0 = \eta_2(1-\varepsilon)$ with $0 < \varepsilon << 1$. Then :

$$E_a \approx R\frac{T_1 \times T_2}{T_2 - T_1} \left[\mathrm{Ln}\left(\frac{\left(\frac{p_2}{\tau_2}\right)}{\left(\frac{p_1}{\tau_1}\right)} \right) + \left(\frac{p_2+1}{p_2} \right) \times \mathrm{Ln}(\varepsilon) - \left(\frac{p_1+1}{p_1} \right) \times \mathrm{Ln}\left(-\mathrm{Ln}\left(\frac{\eta_2}{\eta_1} \right) \right) \right].$$

Thus as $\varepsilon \to 0^+$, $E_a \approx R\frac{T_1 \times T_2}{T_2 - T_1} \left[\left(\frac{p_2+1}{p_2} \right) \times \mathrm{Ln}(\varepsilon) \right] \to -\infty$.

In case $\eta_1 < \eta_2$, as h_0 tends to η_1, we write $h_0 = \eta_1(1-\varepsilon)$ with $0 < \varepsilon << 1$. Then :

$$E_a \approx R\frac{T_1 \times T_2}{T_2 - T_1} \left[\mathrm{Ln}\left(\frac{\left(\frac{p_2}{\tau_2}\right)}{\left(\frac{p_1}{\tau_1}\right)} \right) + \left(\frac{p_2+1}{p_2} \right) \times \mathrm{Ln}\left(-\mathrm{Ln}\left(\frac{\eta_1}{\eta_2} \right) \right) - \left(\frac{p_1+1}{p_1} \right) \times \mathrm{Ln}(\varepsilon) \right].$$

Thus as $\varepsilon \to 0^+$, $E_a \approx R\frac{T_1 \times T_2}{T_2 - T_1} \left[-\left(\frac{p_1+1}{p_1} \right) \times \mathrm{Ln}(\varepsilon) \right] \to +\infty$.

Table 3
Uncertainty on h (in μm):.

h	dh
0.10	0.03
0.20	0.04
0.50	0.07
1.0	0.12
2.0	0.23
5.0	0.80

Since activation energy cannot be infinite, then the only possibility is that $\eta_1 = \eta_2 = \eta$. Then Eq. (16) can be written as:

$$E_a(h=h_0) = R\frac{T_1 \times T_2}{T_2 - T_1} \mathrm{Ln}\left(\frac{\left(\frac{p_2}{\tau_2}\right)}{\left(\frac{p_1}{\tau_1}\right)} \left(-Ln\left(\frac{h_0}{\eta} \right) \right)^{\left(\frac{p_2+1}{p_2} - \frac{p_1+1}{p_1} \right)} \right).$$

Again, as h_0 tends to η, we write $h_0 = \eta(1-\varepsilon)$ with $0 < \varepsilon << 1$. Then :

$$E_a \approx R\frac{T_1 \times T_2}{T_2 - T_1} \mathrm{Ln}\left(\frac{\left(\frac{p_2}{\tau_2}\right)}{\left(\frac{p_1}{\tau_1}\right)} (\varepsilon)^{\left(\frac{1}{p_2} - \frac{1}{p_1} \right)} \right).$$

Thus if $p_1 > p_2$, as $\varepsilon \to 0^+$, $E_a \to -\infty$; otherwise, if $p_1 < p_2$, $E_a \to +\infty$. We conclude that the only possibility is that $p_1 = p_2 = p$.

As a conclusion, if Eq. (14) can be used to fit the sets of experimental data (reacted thickness) at two different temperatures T_1 and T_2, the only case for which the activation energy does not tend to $\pm\infty$ is when $\eta_1 = \eta_2 = \eta$ and $p_1 = p_2 = p$. These hypotheses have been retained in this study.

References

[1] G.J. Verbeck, R.A. Helmuth, Structures and physical properties of cement pastes, Proceedings of the 5th International Symposium on the Chemistry of Cement, Tokyo, 1968.
[2] J.K. Kim, S.H. Han, Y.C. Song, Effect of temperature and aging on the mechanical properties of concrete: part I. Experimental results, Cem. Concr. Res. 32 (2002) 1087–1094.
[3] B. Lothenbach, C. Alder, F. Winnefeld, P. Lunk, Einfluss der Temperatur und Lagerungsbedingungen auf die Festigkeitsentwicklung von Mörteln und Betonen, Beton 55 (12) (2005) 604–609.
[4] M. Zajac, S. Garrault, A. Nonat, Effect of the hydration temperature on mechanical resistance of Portland cement mortar and paste, Cement Wapno Beton 2 (2007) 68–75.
[5] E. Gallucci, X. Zhang, K. Scrivener, Quantitative microstructural study of the effect of temperature on the properties of concrete, International Conference on the Chemistry of Cement, Montreal, 2007.
[6] E. Gallucci, X. Zhang, K. Scrivener, Influence de la température sur le développement microstructural des bétons, (in French), Proceedings of Septième édition des Journées scientifiques du Regroupement francophone pour la recherche et la formation sur le béton (RF)2B, Toulouse, , 2006.
[7] V. Alunno-Rossetti, G. Chiocchio, M. Collepardi, Low pressure steam hydration of tricalcium silicate, Cem. Concr. Res. 4 (1974) 279–288.
[8] K.O. Kjellsen, R.J. Detwiler, O.E. Gjorv, Backscattered electron imaging of cement pastes hydrated at different temperatures, Cem. Concr. Res. 20 (1990) 308–311.
[9] K.O. Kjellsen, R.J. Detwiler, O.E. Gjorv, Pore structure of plain cement pastes hydrated at different temperatures, Cem. Concr. Res. 20 (1990) 927–933.
[10] K.O. Kjellsen, R.J. Detwiler, O.E. Gjorv, Development of microstructures in plain cement pastes hydrated at different temperatures, Cem. Concr. Res. 21 (1991) 179–189.
[11] K.O. Kjellsen, R.J. Detwiler, Reaction kinetics of Portland cement mortars hydrated at different temperatures, Cem. Concr. Res. 22 (1992) 112–120.
[12] K. Asaga, M. Ishizaki, S. Takahashi, K. Konishi, T. Tsurumi, M. Daimon, Effect of curing temperature on the hydration of Portland cement compounds, Proceedings of the 9th International Congress on the Chemistry of Cement, New Delhi, 1992, pp. 181–187.
[13] J.I. Escalante-Garcia, Nonevaporable water from neat OPC and replacement materials in composite cements hydrated at different temperatures, Cem. Concr. Res. 33 (11) (2003) 1883–1888.
[14] J.I. Escalante-Garcia, J.H. Sharp, Effect of temperature on the hydration of the main clinker phases in Portland cements. Part I: neat cements, Cem. Concr. Res. 28 (9) (1998) 1245–1257.
[15] J.I. Escalante-Garcia, J.H. Sharp, Effect of temperature on the hydration of the main clinker phases in Portland cements: part II: blended cements, Cem. Concr. Res. 28 (1998) 1259–1274.
[16] I. Elkhadiri, F. Puertas, The effect of curing temperature on sulphate-resistant cement hydration and strength, Construct. Build Mater. 22 (7) (2008) 1331–1341.
[17] A. Plassais, M.P. Pomies, N. Lequeux, P. Boch, J.P. Korb, D. Petit, F. Barberon, Micropore size analysis by NMR in hydrated cement, Proceedings of the Sixth International Meeting on Recent Advances in Magnetic Resonance Applications to Porous Media, 21(3–4), 2003, pp. 369–371.
[18] L. Lidstrom, B. Westerberg, Fine ground cement in concrete — properties and prospects, ACI Materials J. 5 (2003) 398–406.
[19] D. Bentz, G. Sant, J. Weiss, Early-age properties of cement-based materials. I: influence of cement fineness, J. Mater. Civ. Eng. (2008) 502–508.
[20] B. Osbaeck, V. Johansen, Particle size distribution and rate of strength development of Portland cement, J. Am. Ceram. Soc. 72 (2) (1989) 197–201.

[21] K.M. Alexander, The relationship between strength and the composition and fineness of cement, Cem. Concr. Res. 2 (6) (1972) 663–680.
[22] S. Garrault, T. Behr, A. Nonat, The formation of the C–S–H layer during early hydration of tricalcium silicate grains with different sizes, J. Phys. Chem. B 110 (2006) 270–275.
[23] M. Costoya, Kinetics and microstructural investigation on the hydration of tricalcium silicate, PhD. Thesis, École Polytechnique Fédérale de Lausanne, Switzerland (2008).
[24] K.L Scrivener, The development of microstructure during the hydration of Portland cement, PhD Thesis, Imperial College of Science (1984).
[25] F.O. Anderegg, D.S. Hubbell, The rate of hydration of cement clinker, Proc. Am. Soc. Test. Mater. 29, 554 (1929); 30 572 (1930); cited by H.-F.-W. Taylor, Cement chemistry, 2nd edition, Thomas Telford Ltd Ed. (1997).
[26] T. Knudsen, Modelling hydration of Portland cement, the effect of particle size distribution, Proceedings of the Engineering Foundation Conference on Characterization and Performance Prediction of Cement and Concrete, Henniker, 1982, pp. 125–149.
[27] T. Knudsen, The dispersion model for hydration of Portland cement I. General concepts, Cem. Concr. Res. 14 (5) (1984) 622–630.
[28] J.M. Pommersheim, Effect of particle size distribution on hydration kinetics, Mater. Res. Soc. Symp. Proc. 85 (1987) 301–306.
[29] P.W. Brown, Effects of particle size distribution on the kinetics of hydration of tricalcium silicate, J. Am. Ceram. Soc. 72 (10) (1989) 1829–1832.
[30] T. Westerlund, S. Karrila, K. Perander, A shrinking unreacted core model for estimating the compressive strength of Portland cement, Cem. Concr. Res. 15 (6) (1985) 959–963.
[31] K. van Breugel, Numerical simulation of hydration and microstructural development in hardening cement-based materials (I) theory, Cem. Concr. Res. 25 (2) (1995) 319–331.
[32] D.P. Bentz, E.J. Garboczi, C.J. Haecker, O.M. Jensen, Effects of cement particle size distribution on performance properties of Portland cement-based materials, Cem. Concr. Res. 29 (10) (1999) 1663–1671.
[33] E. Guillon, J. Chen, G. Chanvillard, Physical & chemical modeling of the hydration kinetics of OPC paste using a semi-analytical approach, Proceedings of ConMod'08, Delft, 2008, pp. 165–172.
[34] S. Bishnoi, K.L. Scrivener, μic: a new platform for modelling the hydration of cements, Cem. Concr. Res. 39 (4) (2009) 266–274.
[35] F. Tomosawa, 10th Int. Congr. Chem. Cement, Goteborg, vol. 2, 1997, p. 2ii051.
[36] L. D'Aloia, G. Chanvillard, Determining the 'apparent' activation energy of concrete: Ea—numerical simulations of the heat of hydration of cement, Cem. Concr. Res. 32 (2002) 1277–1289.
[37] T. Kishi, K. Maekawa, Multi component model for hydration heating Portland cement, Translation from Proceedings of JSCE, No. 526/V-29, , 1995.
[38] F. Lin, C. Meyer, Hydration kinetics modeling of Portland cement considering the effects of curing temperature and applied pressure, Cem. Concr. Res. 39 (4) (2009) 255–265.
[39] A.K. Schindler, Effect of temperature on the hydration of cementitious materials, ACI Mater. J. 101 (1) (2004) 72–81.
[40] IUPAC Compendium of Chemical Terminology, The Gold Book, in: A.D. McNaught, A. Wilkinson (Eds.), Second ed., Blackwell Science, 1997.
[41] D. Swartzendruber, S.A. Barber, Dissolution of limestone particles in soil, Soil Sci. 100 (4) (1965) 287–291.
[42] B. Lothenbach, T. Matschei, G. Möschner, F. Glasser, Thermodynamic modelling of the effect of temperature on the hydration and porosity of Portland cement, Cem. Concr. Res. 38 (1) (2008) 1–18.
[43] H.F.W. Taylor, Cement Chemistry, 2nd ed. Thomas Telford Ltd Ed., 1997
[44] F. Ridi, E. Fratini, F. Manelli, P. Baglioni, Hydration process of cement in the presence of a cellulosic additive. A calorimetric investigation, J. Phys. Chem. B 109 (2005) 14727–14734.
[45] L.E. Copeland, D.L. Kantro, Hydration of Portland cement, Proc 5th International Congress on the Chemistry of Cement, Tokyo, 1968, pp. 387–420.
[46] S. Swaddiwudhipong, D. Chen, M.H. Zhang, Simulation of the exothermic process of Portland cement, Adv. Cem. Res. 14 (2) (2002) 61–69.
[47] A. Damasceni, E. Dei, L. Fratini, F. Ridi, S.H. Chen, P. Baglioni, A novel approach based on differential scanning calorimetry applied to the study of tricalcium silicate hydration kinetics, J. Phys. Chem. B 106 (2002) 11572–11578.
[48] L.J. Parrott, D. Killoh, R. Patel, Cement hydration under partially saturated condition, Proc. 8th Int. Cong. Chemistry of Cement, Rio de Janeiro, 1986, pp. 46–50.
[49] T.C. Powers, T.L. Brownyard, Studies of the Physical Properties of Hardened Portland Cement Paste, Journal of the American Concrete Institute, 43 (multiple parts) 101, 249, 469, 549, 669, 845, 993, 1947, also published as PCA Bulletin 22, Research Laboratories of the Portland Cement Association, Chicago, 1948.